ORAL PRESENTATION

Chaxines from the edible mushroom *Agrocybe chaxingu* are electronically competent Michael acceptors but do not engage the cathepsin K active site: An *in silico* target-deconvolution study

Gamze Altıntaş Kazar[1]* (ORCID: https://orcid.org/0000-0002-0220-0263)

*[1]Trakya University, Faculty of Science, Department of Biology, Edirne, Türkiye.

*Corresponding author e-mail: gamzealtintas@trakya.edu.tr

Abstract

The edible mushroom *Agrocybe chaxingu* produces chaxines, degraded ergostane-type metabolites that suppress osteoclast formation without cytotoxicity, yet their molecular target has never been identified. Because the chaxines carry a cross-conjugated α,β-unsaturated carbonyl and because osteoclast function depends on the cysteine protease cathepsin K, covalent engagement of the catalytic Cys25 is a plausible but untested hypothesis. Chaxines B–E were evaluated against a nine-receptor panel comprising eight osteoclast effectors (cathepsins K, L, S and B, carbonic anhydrase II, MMP-9, c-Src and CSF1R) and RORγt, using AutoDock Vina with three seeds. Every receptor was validated by redocking its own co-crystallised ligand; seven of nine reproduced the crystallographic pose, cathepsin K most accurately at 0.29 Å. The chaxines bound the cathepsin K site at −6.6 to −7.2 kcal/mol and outscored no cognate reference at any interpretable validated target: only MMP-9, whose zinc-chelating hydroxamate reference is systematically underestimated, and cathepsin L, whose reference is a covalent adduct, gave negative values. Electronic-structure calculations placed them in the electrophilicity range of established Michael acceptors and far from the non-electrophilic sterol ergosterol. However, a geometric criterion calibrated against a crystallographic pre-covalent nitrile complex showed the electrophilic β-carbon approaching Cys25 Sγ edge-on. Of 144 poses across four cysteine proteases, twelve came within 4.5 Å, yet none qualified at 30° or 40° from the perpendicular and a single pose appeared only at 50°, beyond the range compatible with conjugate addition. Ensemble docking over nine crystal forms, whole-surface blind docking and orthogonal rescoring reproduced the result. Retrospective validation against 60 known actives and 582 decoys gave a ROC-AUC of 0.602 with no early enrichment: scores carry little information in this pocket, and the conclusion rests on pose geometry rather than affinity. Direct active-site inhibition of cathepsin K is therefore an unlikely explanation for the osteoclast-suppressing phenotype of these mushroom metabolites.

Keywords: chaxine, *Agrocybe chaxingu*, cathepsin K, molecular docking, Michael acceptor, target deconvolution

INTRODUCTION

Edible and medicinal mushrooms remain a productive source of structurally unusual secondary metabolites. The edible mushroom *Agrocybe chaxingu* yields a family of degraded ergostane-type metabolites, the chaxines. Chaxine A was first isolated as an osteoclast-forming suppressing substance (Kawagishi et al., 2006), and chaxines B, C, D and E followed, of which chaxines B and C suppressed osteoclast formation without cytotoxicity (Choi et al., 2009). These compounds are not sterols in the strict sense but seco-steroidal degradation products in which a hydrindanone is linked through an α,β-unsaturated ester bridge to a methylcyclohexenone. Despite a clear bone-protective phenotype, the molecular target underlying their activity has never been defined.

Osteoclast function depends on a small number of druggable effectors: cathepsin K, the principal collagenolytic protease of the resorption lacuna and target of the clinical inhibitor odanacatib (Gauthier et al., 2008; Drake et al., 2017); carbonic anhydrase II, which acidifies the lacuna; MMP-9, which degrades the residual matrix; and the kinases c-Src and CSF1R. The nuclear receptor RORγt (Ivanov et al., 2006) is included as a sterol-binding reference point, Th17 cells acting as an osteoclastogenic helper subset in inflammatory bone loss (Sato et al., 2006).

The electrophilic substitution pattern shared by the chaxines implicates a cysteine protease. All four congeners retain a cross-conjugated α,β-unsaturated carbonyl in which the exocyclic methine carbon is β to a ring ketone and α to an ester, a doubly activated Michael acceptor. Cathepsin K and its paralogues cathepsins L, S and B possess a nucleophilic catalytic cysteine, and inhibition of this family proceeds almost exclusively through covalent or covalent-reversible chemistry at that residue. Conjugate addition of Cys25 to the chaxine enone is therefore a mechanistically defined hypothesis that structure-based calculation can evaluate prior to experiment.

Chaxines B–E were therefore evaluated by structure-based docking into a nine-receptor panel, each receptor validated by redocking its own co-crystallised ligand; by a geometric criterion for covalent compatibility calibrated against a crystallographic pre-covalent complex; by semi-empirical quantum-chemical descriptors of electrophilicity; and by four robustness tests: ensemble docking, whole-surface blind docking, orthogonal rescoring and retrospective validation against known actives.

MATERIALS AND METHODS

Receptor panel and structure preparation

X-ray crystal structures of the human target proteins were retrieved from the Protein Data Bank (Berman et al., 2000) by UniProt accession, restricted to entries of 2.5 Å resolution or better with a non-polymer entity. Candidate ligands were ranked by burial (protein heavy atoms within 4.5 Å), small components and buffer species discarded, and each selection checked against the chemical-component name so that the retained ligand is the canonical orthosteric reference.

The co-crystallised inhibitors of the cysteine cathepsins proved to be almost exclusively covalent adducts (ligand-to-Sγ 1.71–1.83 Å), so non-covalent complexes were searched for explicitly. For cathepsin K, entry 4X6I (Borisek et al., 2015) captures a nitrile-bearing inhibitor in a pre-covalent state with its warhead carbon 3.35 Å from Cys25 Sγ, and was selected as the primary receptor because it provides a crystallographic calibration point for electrophile positioning. For cathepsin L no non-covalent complex exists and the covalent reference was retained, its covalency flagged in Table 1. For cathepsin B the best available complex was used; its reference is a peptidomimetic carbamate deposited with its leaving group intact.

Chain A was retained (chain D for cathepsin S), the co-crystallised ligand and waters removed, alternate conformations other than A discarded, and catalytic or structural ions within 12 Å of the site kept. Protonation was assigned at pH 7.4 with Open Babel 3.2.1 (O'Boyle et al., 2011) and receptors were treated as rigid. The catalytic cysteine was modelled as the neutral thiol rather than the thiolate of the Cys–His ion pair; because the analysis reported here is geometric and the sulfur position is unchanged by protonation state, this affects the electrostatic term of the score but not the measured approach geometry.

Ligand set

Chaxines B–E were retrieved from PubChem and verified by exact InChIKey matching (Kim et al., 2023). Each chaxine carries six or seven stereocentres, of which two side-chain centres are undefined in the deposited records; the deposited stereochemistry was used throughout. Ergosterol served as a fungal sterol baseline, with odanacatib, E-64, CA-074, acetazolamide, marimastat, dasatinib and pexidartinib as target-matched references. Coordinates were generated with RDKit 2024.03.6 (ETKDGv3 then MMFF), protonated at physiological pH and converted to PDBQT with Meeko 0.8.0 (Landrum et al., 2024).

Molecular docking and protocol validation

Docking used AutoDock Vina 1.2.7 with a 20 Å cubic box centred on the heavy-atom centroid of each receptor's co-crystallised ligand, an exhaustiveness of 8, nine poses retained per run and three independent runs (seeds 42, 7 and 123); affinities are reported as mean and standard deviation of the top-ranked pose, and seed-to-seed convergence is reported (Trott and Olson, 2010; Eberhardt et al., 2021). Before any test compound was evaluated, each receptor was validated by redocking its own co-crystallised ligand, taken as three-dimensional coordinates with bond orders from the RCSB ModelServer, and computing the heavy-atom RMSD of the best-scoring pose by element-matched nearest-neighbour assignment; an RMSD below 2 Å was taken as successful reproduction of the experimental binding mode.

Because empirical scoring functions are not calibrated between binding sites, raw affinities are not compared across targets; each ligand is reported relative to that target's own redocked cognate ligand (ΔΔG).

Covalent-compatibility geometry

For each docked pose in the four cysteine proteases the Michael acceptor was located by substructure matching, preferring the ketone-activated system, and two quantities measured between the electrophilic β-carbon and the catalytic sulfur: the heavy-atom distance, and the deviation of the S···Cβ vector from the normal to the enone plane, which expresses how far the approach departs from the perpendicular trajectory towards the π* lobe of Cβ that conjugate addition requires (0° ideal). Four chaxines × four receptors × nine poses of the seed-42 run give the 144 poses analysed. Cathepsin B is included although it failed the redocking criterion, because the quantity measured is pose geometry rather than score; excluding it would only remove candidate geometries.

Two calibrations were applied. The distance scale was calibrated on the cognate nitrile of 4X6I, measured both in the crystal and after redocking, which quantifies how far the non-covalent protocol displaces a warhead known to be correctly positioned. The calibration applies to distance only: a nitrile carbon is sp-hybridised and has no enone plane, so it cannot calibrate an angular threshold. The angular criterion is therefore taken from the stereoelectronic requirement of conjugate addition, and because that threshold is a choice, qualifying poses are counted across a range of cut-offs rather than at a single value.

Electronic-structure descriptors

Geometries were optimised with GFN2-xTB and frontier-orbital energies extracted (Bannwarth et al., 2019). The chemical potential was taken as $\mu = (E_{HOMO} + E_{LUMO})/2$, the hardness as $\eta = E_{LUMO} - E_{HOMO}$, and the global electrophilicity index as $\omega = \mu^2/(2\eta)$ (Parr et al., 1999). Dimethyl fumarate, helenalin and curcumin were included as reference Michael acceptors, acrylamide as a weak acceptor and ergosterol as a non-electrophilic control. Absolute values from a semi-empirical method are not comparable with published DFT values, and the global index is used only to separate electrophiles from non-electrophiles, not to rank reactivity within the electrophile class.

Robustness tests and retrospective validation

Ensemble docking repeated the protocol in nine further cathepsin K crystal forms, whose accession codes are listed with the deposited data. Whole-surface blind docking used a 57 Å box enclosing the protein with exhaustiveness 32 and twenty poses in each of three runs, each pose classified as active-site or ectosteric by whether its centroid lay within 10 Å of Cys25 Sγ. The top-ranked Vina pose of every pair was rescored with Vinardo and normalised as ligand and lipophilic efficiency; AD4 requires AutoGrid maps which are unavailable, so one orthogonal function was used (Quiroga and Villarreal, 2016).

Bioactivity records for human cathepsin K (ChEMBL target CHEMBL268) were retrieved for IC50, Ki, Kd and EC50 endpoints with a pChEMBL value; records with a data-validity comment, non-human records and imprecise relations were removed and a median taken per molecule, giving 2,227 molecules of which 1,151 have pChEMBL ≥ 7 (Mendez et al., 2019). Sixty structurally diverse actives were chosen by MaxMin picking on ECFP4 fingerprints. Decoys came from a 24,990-molecule ChEMBL background set excluding any molecule with recorded activity against the target, matched to each active on molecular weight, cLogP, hydrogen-bond donors, acceptors and rotatable bonds, with Tanimoto similarity below 0.35 to every active; 582 decoys resulted, a ratio of 9.7 per active rather than the 50:1 of DUD-E, which widens the uncertainty on the enrichment factors. This screen was a single pass (seed 42, five poses) and is kept separate from the three-seed panel means throughout. Discrimination was quantified by ROC-AUC, enrichment factors and the Spearman correlation between score and pChEMBL.

Table 1. Receptor panel and protocol validation.

Target	PDB	Res. (Å)	Cognate ligand	Covalent	RMSD (Å)	Validated
CTSK	4X6I	1.87	3Y1	False	0.29	yes
CTSL	2XU3	0.90	XU3	True	1.93	yes
CTSS	4P6G	1.58	2FZ	False	0.51	yes
CTSB	8B4T	1.45	P9F	False	2.39	no
CA2	3HS4	1.10	AZM	False	3.07	no
MMP9	4XCT	1.30	N73	False	0.65	yes
SRC	7NG7	1.50	UCW	False	1.83	yes
CSF1R	6IG8	1.80	A7O	False	1.49	yes
RORGT	9N9L	1.64	A1BW2	False	1.50	yes

(Each receptor was validated by redocking its own co-crystallised ligand; RMSD below 2 Å was taken as success. Covalent indicates a deposited covalent adduct; the cathepsin B reference P9F is deposited with its 4-chlorophenoxycarbonyl group intact and is not scored as one.)

RESULTS

Protocol validation

Seven of the nine receptors reproduced their crystallographic binding mode (Table 1); the median RMSD across the nine was 1.50 Å. Cathepsin K, which carries the primary hypothesis, was the most accurate at 0.29 Å. Two failed and are excluded from the affinity comparison: carbonic anhydrase II (3.07 Å), because the zinc coordination of the sulfonamide reference is not modelled, and cathepsin B (2.39 Å), whose peptidomimetic reference the rigid protocol did not reproduce. The RORγt control redocked at 1.50 Å.

Seed-to-seed convergence was high: the median standard deviation of the top-ranked score was 0.010 kcal/mol for the redocking controls, 0.040 across the 108 ligand-target pairs and 0.067 in the cathepsin K column.

The chaxines do not prefer cathepsin K

Against the validated cathepsin K receptor the chaxines scored between −6.63 and −7.21 kcal/mol, weaker than the fungal sterol ergosterol (−7.24 kcal/mol), the clinical cathepsin K inhibitor odanacatib (−7.44 kcal/mol) and the receptor's own co-crystallised ligand (−7.65 kcal/mol). These differences are small, and the retrospective validation reported below shows that scores in this pocket cannot be read as a potency ranking.

Expressed relative to each target's cognate ligand (Table 2), the chaxines are 0.44–1.02 kcal/mol weaker than the reference at cathepsin K. The most negative ΔΔG values belong to the two receptors that failed validation — carbonic anhydrase II (−1.43 to −2.17) and cathepsin B (−0.84 to −1.67) — and are not interpreted. Among validated targets MMP-9 is clearly negative (−0.11 to −1.26), where the reference N73 (ARP101) is a zinc-chelating hydroxamate underestimated for the same reason acetazolamide is. At cathepsin L the column spans −0.02 to +0.30, so one chaxine is level with the reference; that reference is a covalent adduct and its redocking RMSD of 1.93 Å is the weakest that passed, so this column is not interpreted either.

Electronically competent, geometrically incompatible

The electronic descriptors place the chaxines among the electrophiles. Their LUMO energies lie between −7.89 and −8.02 eV and their electrophilicity indices between 16.0 and 17.0 eV, within the range spanned by dimethyl fumarate (17.7 eV), curcumin (18.9 eV) and helenalin (15.5 eV), and far from the non-electrophilic control ergosterol (9.4 eV) and the weak acceptor acrylamide (10.9 eV). The index does not order reactivity within the electrophile class in which it places curcumin above dimethyl fumarate, the stronger thiol acceptor, so it is used only for the separation it supports.

Reactivity is not the limiting factor but positioning is.

In the crystal, the nitrile warhead of the cathepsin K reference sits 3.35 Å from Cys25 Sγ; redocked under the present non-covalent protocol the same warhead settles at 4.75–4.79 Å across all three seeds, a systematic displacement of about 1.4 Å. Measured against that calibration the chaxines are not distant from the catalytic sulfur: their electrophilic β-carbon reaches 3.92–4.08 Å in the closest pose at cathepsin K, closer than the

redocked reference itself. The approach trajectory, however, is wrong: at the closest approach the deviation from the perpendicular attack vector is 62.5–70.1°, so the sulfur lies close to the plane of the enone rather than above it.

Across the four cysteine proteases 144 poses were examined. Most lie well away from the catalytic sulfur — in the top-ranked poses at cathepsin K the β-carbon is 6.22–12.20 Å distant — and twelve came within 4.5 Å, spanning deviations of 45.2–90.0°. The conclusion does not depend on where the angular threshold is placed: counted cumulatively at the 4.5 Å cut-off, 0, 0, 1, 1 and 8 poses qualify at 30°, 40°, 50°, 60° and 70° respectively, so the first qualifying pose appears only at 50°, by which point the trajectory is already too far from perpendicular for conjugate addition (Figure 1).

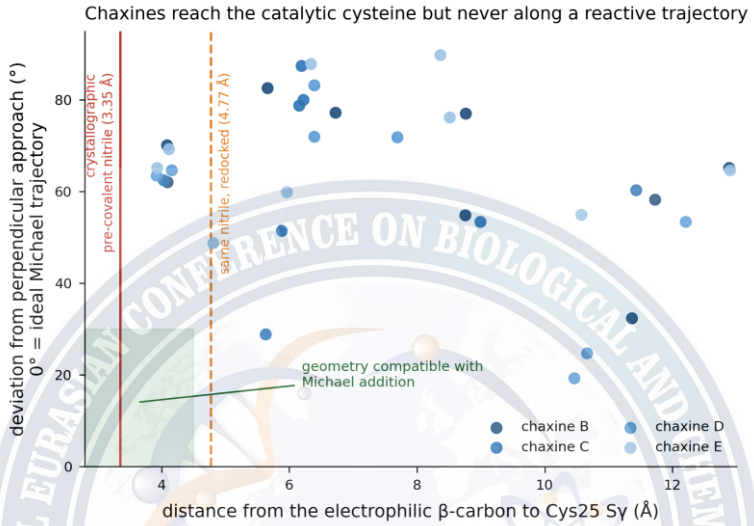


Figure 1. Covalent-compatibility geometry at cathepsin K.

(Each point is one docked pose. The shaded region marks the strictest criterion applied (within 4.5 Å and 30° of the perpendicular); no pose falls within it, and the full threshold sweep from 30° to 70° is reported in the text. The solid line is the crystallographic pre-covalent nitrile of PDB 4X6I and the dashed line the same warhead after redocking, which defines the systematic offset of the protocol.)

Robustness tests

Ensemble docking across nine further cathepsin K crystal forms left the picture unchanged. Averaged over the ensemble the chaxines score −6.48 to −6.99 kcal/mol, indistinguishable from ergosterol (−6.99) and odanacatib (−6.96), and the spread between crystal forms (SD 0.18–0.34 kcal/mol) is as large as the differences between compounds. Individual chaxines outscore one or other reference in some structures (chaxines B and C in four and five of the nine forms, chaxine E in none).

Whole-surface blind docking showed no preference for the catalytic site: only 13–37 per cent of chaxine poses fell within 10 Å of Cys25 Sγ, and for chaxines C, D and E the best pose over the entire surface lay outside that radius (10.4–11.1 Å). Odanacatib placed 58 per cent of its poses in the active site.

Orthogonal rescoring with Vinardo agreed closely with Vina over the 108 ligand-target pairs (Spearman ρ = 0.888), and under neither function was cathepsin K the preferred target of any chaxine. Ligand efficiency at cathepsin K was 0.203–0.224 kcal/mol per heavy atom, below ergosterol (0.250), and lipophilic efficiency ranged from −1.40 to 0.05, indicating that what score they achieve is driven largely by lipophilicity.

For orientation only, assays of this class were run over roughly 0.2–3.2 µg/mL (Kawagishi et al., 2006; Choi et al., 2009), about 0.4–7.3 µM for chaxines B–E, while their cathepsin K scores imply dissociation constants of 5.2–13.9 µM at 298 K. Cellular potency is not target affinity, so the comparison is indicative.

The fourth test: the protocol reproduces poses but cannot rank potency

Against sixty structurally diverse known cathepsin K actives and 582 property-matched decoys the protocol reached a ROC-AUC of 0.602 (Figure 2). Enrichment was absent in the top one per cent and marginal thereafter

(enrichment factors 0.00, 0.65 and 1.15 at 1, 5 and 10 per cent). The correlation between docking score and measured pChEMBL was in the expected direction but weak and not significant (Spearman ρ = −0.239, p = 0.066, n = 60). The score distributions of actives (median −6.98 kcal/mol) and decoys (median −6.78 kcal/mol) overlap almost completely.

The positive control locates the problem precisely. Odanacatib scores −7.41 kcal/mol, stronger than 73 per cent of the known actives but also than 82 per cent of the decoys: the function ranks it well, yet it ranks a large fraction of presumed-inactive compounds almost as well. The chaxines fall in the same undifferentiated band, chaxine B at −7.27 kcal/mol ranking above 62 per cent of actives and chaxine E at −6.54 kcal/mol above 18 per cent. Their position in this distribution carries no information about inhibition, and no conclusion here rests on affinity differences.

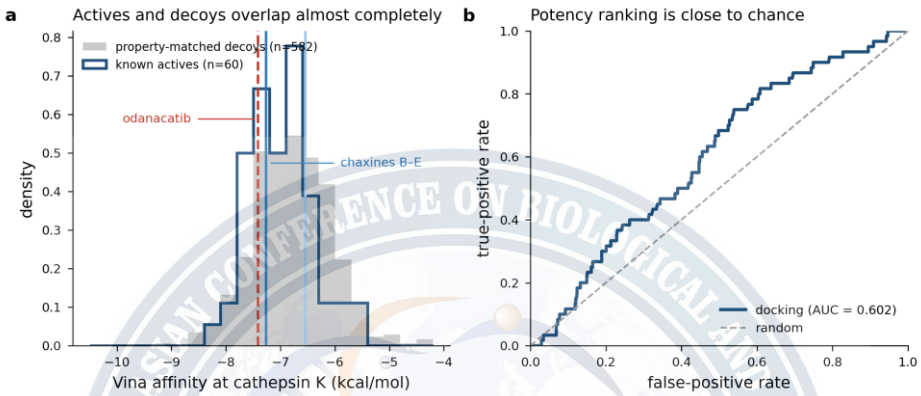


Figure 2. Retrospective validation at cathepsin K. (a) Docking scores of 60 known actives, 582 property-matched decoys and the test compounds. (b) ROC curve for the separation of actives from decoys.

Table 2. Affinity relative to each target's own co-crystallised ligand (ΔΔG, kcal/mol); subset of the full ligand set, the remainder being deposited with the data.

Ligand	CTSK	CTSL	CTSS	MMP9	SRC	CSF1R	RORGT	CTSB	CA2
Chaxine_B	0.44	0.0	0.24	-0.75	1.69	3.11	0.78	-1.05	-2.17
Chaxine_C	0.49	0.19	0.21	-1.26	1.53	2.63	1.41	-1.67	-2.1
Chaxine_D	0.94	-0.02	0.34	-0.11	1.48	2.39	1.07	-1.23	-1.43
Chaxine_E	1.02	0.3	1.07	-0.15	2.1	3.17	1.2	-0.84	-1.62
Ergosterol	0.41	-0.06	0.81	-0.31	1.98	3.38	0.69	-1.3	-1.61
Odanacatib	0.21	0.24	0.93	-1.97	0.22	2.59	1.24	-0.7	-2.93

(Positive values indicate weaker binding than the cognate reference. The last two columns failed redocking validation (Table 1) and are shown only because they carry the most negative values in the panel; they are not interpreted.)

DISCUSSION

The hypothesis under test was narrow and chemically motivated: covalent modification of the catalytic cysteine of cathepsin K by the chaxines. The results do not support it, and the manner of the failure is informative. Electrophilicity is not the limiting factor; by frontier-orbital criteria the chaxines fall among established Michael acceptors, one in clinical use. The limitation is geometric. In none of the poses examined is the electrophile presented to Cys25 within the angular range compatible with conjugate addition. The two properties could be resolved separately only because each was measured independently, which indicates that electrophilicity alone is an inadequate criterion for prioritising natural-product Michael acceptors against cysteine enzymes. Calibration was equally essential: a β-carbon 3.9–4.1 Å from a catalytic sulfur acquires meaning only once the same protocol is known to place an observed pre-covalent nitrile at 4.75 Å rather than 3.35 Å.

The conclusion rests on the approach geometry of the electrophile, and reproduction of experimental poses is what the protocol was shown to do well (0.29 Å at cathepsin K). The positional result (a preference for sites remote from the catalytic cleft) and the invariance of both observations across nine crystal forms are consistent

with that interpretation, but each depends on the subset of poses selected by the scoring function and is therefore corroborative rather than decisive. No weight is placed on the affinity data: a ROC-AUC of 0.602 with no enrichment in the top one per cent indicates that known inhibitors and property-matched decoys receive interchangeable scores in this pocket.

Five limitations constrain these conclusions. Scoring functions discriminate potency only weakly here. The receptors were held rigid, and the catalytic cysteine was modelled as the neutral thiol rather than the catalytically relevant thiolate. The two undefined side-chain stereocentres were retained as deposited. The decoy set falls below the 50:1 ratio of benchmark collections. Most consequentially, a non-covalent protocol interrogates only whether the recognition step is accessible among the selected poses; the decisive calculation, docking under a distance restraint between the β-carbon and Cys25 Sγ, or covalent docking with a QM/MM treatment of the addition step, has not been undertaken.

If cathepsin K is not the target, the cysteines of the RANKL–NF-κB signalling axis are the most plausible alternatives. Dimethyl fumarate and helenalin, the two reference acceptors nearest the chaxines in electrophilicity, act through Keap1 and through the p65 subunit of NF-κB respectively, and both pathways converge upon osteoclast differentiation. Application of the calibrated geometric criterion to that target set constitutes the direct extension of this work.

CONCLUSION

Chaxines B–E are electronically competent Michael acceptors, clearly distinct from the non-electrophilic sterol ergosterol, yet they do not engage the cathepsin K active site. Of the 144 poses examined, none combines proximity to the catalytic cysteine with a trajectory compatible with conjugate addition: no pose qualifies at 30° or 40° and the first appears only at 50°. Neither this nor the absence of any preference for the catalytic site changes across nine crystal forms, and the conclusion does not depend on docking scores. Priority in subsequent work therefore falls to the cysteine-rich signalling proteins of the RANKL–NF-κB axis.

ACKNOWLEDGEMENTS

This study received no specific grant from any funding agency. The author declares no competing interests.
All structures used are public Protein Data Bank entries and all bioactivity data are public ChEMBL records; accession codes are given in Table 1 and in the Methods. The analysis scripts, prepared receptor and ligand files, all docking poses and the complete result tables underlying every figure including the per-target panel, the ensemble and blind-docking runs with their accession codes, the angular threshold sweep and the retrospective validation set will be available from the author on request.

REFERENCES

Bannwarth, C., Ehlert, S., & Grimme, S. (2019). GFN2-xTB—an accurate and broadly parametrized self-consistent tight-binding quantum chemical method with multipole electrostatics and density-dependent dispersion contributions. Journal of Chemical Theory and Computation, 15(3), 1652-1671.

Berman, H. M., Westbrook, J., Feng, Z., Gilliland, G., Bhat, T. N., Weissig, H., Shindyalov, I. N., & Bourne, P. E. (2000). The Protein Data Bank. Nucleic Acids Research, 28(1), 235-242.

Borisek, J., Vizovisek, M., Sosnowski, P., Turk, B., Turk, D., Mohar, B., & Novic, M. (2015). Development of N-(functionalized benzoyl)-homocycloleucyl-glycinonitriles as potent cathepsin K inhibitors. Journal of Medicinal Chemistry, 58(17), 6928-6937.

Choi, J. H., Ogawa, A., Abe, N., Masuda, K., Koyama, T., Yazawa, K., & Kawagishi, H. (2009). Chaxines B, C, D, and E from the edible mushroom Agrocybe chaxingu. Tetrahedron, 65(48), 9850-9853.

Drake, M. T., Clarke, B. L., Oursler, M. J., & Khosla, S. (2017). Cathepsin K inhibitors for osteoporosis: biology, potential clinical utility, and lessons learned. Endocrine Reviews, 38(4), 325-350.

Eberhardt, J., Santos-Martins, D., Tillack, A. F., & Forli, S. (2021). AutoDock Vina 1.2.0: new docking methods, expanded force field, and Python bindings. Journal of Chemical Information and Modeling, 61(8), 3891-3898.

Gauthier, J. Y., Chauret, N., Cromlish, W., Desmarais, S., Duong, L. T., Falgueyret, J. P., ... & Black, W. C. (2008). The discovery of odanacatib (MK-0822), a selective inhibitor of cathepsin K. Bioorganic & Medicinal Chemistry Letters, 18(3), 923-928.

Ivanov, I. I., McKenzie, B. S., Zhou, L., Tadokoro, C. E., Lepelley, A., Lafaille, J. J., Cua, D. J., & Littman, D. R. (2006). The orphan nuclear receptor RORγt directs the differentiation program of proinflammatory IL-17+ T helper cells. Cell, 126(6), 1121-1133.

Kawagishi, H., Akachi, T., Ogawa, T., Masuda, K., Yamaguchi, K., Yazawa, K., & Takahashi, M. (2006). Chaxine A, an osteoclast-forming suppressing substance, from the mushroom Agrocybe chaxingu. Heterocycles, 69, 253-258.

Kim, S., Chen, J., Cheng, T., Gindulyte, A., He, J., He, S., ... & Bolton, E. E. (2023). PubChem 2023 update. Nucleic Acids Research, 51(D1), D1373-D1380.

Landrum, G., Tosco, P., Kelley, B., Rodriguez, R., Cosgrove, D., Vianello, R., ... & strets123. (2024). rdkit/rdkit: 2024_03_6 (Q1 2024) release (Version Release_2024_03_6) [Computer software]. Zenodo. https://doi.org/10.5281/zenodo.13469390

Mendez, D., Gaulton, A., Bento, A. P., Chambers, J., De Veij, M., Felix, E., ... & Leach, A. R. (2019). ChEMBL: towards direct deposition of bioassay data. Nucleic Acids Research, 47(D1), D930-D940.

O'Boyle, N. M., Banck, M., James, C. A., Morley, C., Vandermeersch, T., & Hutchison, G. R. (2011). Open Babel: an open chemical toolbox. Journal of Cheminformatics, 3, 33.

Parr, R. G., Szentpaly, L. v., & Liu, S. (1999). Electrophilicity index. Journal of the American Chemical Society, 121(9), 1922-1924.

Quiroga, R., & Villarreal, M. A. (2016). Vinardo: a scoring function based on AutoDock Vina improves scoring, docking, and virtual screening. PLoS ONE, 11(5), e0155183.

Sato, K., Suematsu, A., Okamoto, K., Yamaguchi, A., Morishita, Y., Kadono, Y., ... & Takayanagi, H. (2006). Th17 functions as an osteoclastogenic helper T cell subset that links T cell activation and bone destruction. Journal of Experimental Medicine, 203(12), 2673-2682.

Trott, O., & Olson, A. J. (2010). AutoDock Vina: improving the speed and accuracy of docking with a new scoring function, efficient optimization, and multithreading. Journal of Computational Chemistry, 31(2), 455-461.